Materials Chemistry and Physics 113 (2009) 690–695

Contents lists available at ScienceDirect

Materials Chemistry and Physics

journal homepage: www.elsevier.com/locate/matchemphys

Optical constants of thermally evaporated Se–Sb–Te films using only their transmission spectra

K.A. Aly[a,*], H.H. Amer[b], A. Dahshan[c]

[a] Physics Department, Faculty of Science, Al-Azhar University, Assiut Branch, Assiut 71511, Egypt
[b] Solid State Physics Department, National Center for Radiation Research and Technology, Atomic Energy Authority, Cairo, Egypt
[c] Department of Physics, Faculty of Science, Suez Canal University, Port Said, Egypt

ARTICLE INFO

Article history:
Received 28 May 2008
Received in revised form 5 August 2008
Accepted 12 August 2008

Keywords:
Thin films
Thermal evaporation
Optical constants

ABSTRACT

Amorphous $Se_{82-x}Te_{18}Sb_x$ thin films with different compositions (x = 0, 3, 6 and 9 at.%) were deposited onto glass substrates by thermal evaporation. The transmission spectra, $T(\lambda)$, of the films at normal incidence were obtained in the spectral region from 400 to 2500 nm. Based on the use of the maxima and minima of the interference fringes, a straightforward analysis proposed by Swanepoel has been applied to derive the optical constants and the film thickness. The dispersion of the refractive index is discussed in terms of the single-oscillator Wemple and DiDomenico model. Tauc relation for the allowed non-direct transition describes the optical transition in the studied films. With increasing antimony content the refractive index increases while the optical band gap decreases. The optical band gap decreases from 1.62 to 1.26 eV with increasing antimony content from 0 to 9 at.%. The chemical-bond approach has been applied successfully to interpret the decrease of the optical gap with increasing antimony content.

1. Introduction

The increasing interest in the investigations of chalcogenide semiconducting glasses has been determined by their unique properties of importance not only for practical applications but also for understanding of the nature of the physical processes in them. Both selenium and tellurium are expected to be important semiconductor elements, because of their possible application in the fabrication of semiconductor devices.

Glassy alloys of Se–Te system based on Se have become materials of considerable commercial, scientific and technological importance. They are widely used for various applications in many fields as optical recording media because of their excellent laser writer sensitivity, xerography, and electrographic applications such as photoreceptors in photocopying and laser printing [1–3]. Amorphous Se–Te alloys have greater hardness, higher crystallization temperature, higher photosensitivity and smaller ageing effects than pure Se [4].

The addition of Sb to the chalcogenide glasses expands the glass forming area and also creates compositional and configurational disorder in the system [5–7]. The energy band gap of the material plays a major role in the preparation of the device for a particular wavelength, which can be modified by the addition of impurity [8]. So, the influence of metallic additives on the optical properties has been an important issue in the case of chalcogenide glasses.

The present paper reports the effect of Sb additive on the optical properties of thermally evaporated $Se_{82}Te_{18}$ thin films. The well-known Swanepoel's method [9,10] were used for calculating the two (real and imaginary) parts of the refractive index and the film thickness in the weakly absorbing and transparent regions of the transmittance spectra. To the best of our knowledge, there has been no thorough or systematic study on the system under investigation.

2. Experimental details

Different compositions of bulk $Se_{82-x}Te_{18}Sb_x$ (x = 0, 3, 6 and 9 at.%) chalcogenide glasses were prepared from their components of high purity (99.999%) by the melt quench technique. The elements were heated together in an evacuated silica ampoule up to 980 K and then the ampoule temperature kept constant for about 24 h. During the course of heating, the ampoule was shaken several times to maintain the uniformity of the melt. Finally, the ampoule was quenched into ice-cooled water to avoid crystallization.

The amorphous thin films were deposited by evaporating the alloys from a resistance-heat quartz crucible onto clean glass substrates kept at room temperature and a vacuum of about 10^{-3} Pa using a conventional coating unit (Denton Vacuum DV 502 A). The evaporation rate and the film thickness were controlled using a quartz crystal DTM 100 monitor. Mechanical rotation of the substrates during deposition produced homogeneous films. The temperature rise of the substrate due to radiant heating from crucible was negligible. According to Kosa et al. [11] the homogeneity of the thin film samples was clearly confirmed by the corresponding

* Corresponding author. Tel.: +20 126418273; fax: +20 882181436.
E-mail addresses: kamalaly2001@gmail.com (K.A. Aly), adahshan73@gmail.com (A. Dahshan).

0254-0584/$ – see front matter © 2008 Elsevier B.V. All rights reserved.
doi:10.1016/j.matchemphys.2008.08.035

spectral dependence of transmission, where no shrinkage of the interference fringes was observed.

The amorphous state of the films was checked using X-ray (Philips type 1710 with Cu as a target and Ni as a filter, $\lambda = 1.5418$ Å) diffractometer. The absence of crystalline peaks confirms the amorphous state of the prepared samples. The elemental compositions of the investigated specimens were checked using the energy dispersive X-ray (Link Analytical Edx) spectroscopy. The deviations in the elemental compositions of the evaporated films from their initial bulk specimens were found not to exceed 1.0 at.%.

A double beam (Jasco V-630) spectrophotometer was used to measure the transmittance for the prepared films in the spectral range of wavelength from 400 to 2500 nm. Without a glass substrate in the reference beam, the measured transmittance spectra were used to calculate the optical constants of the films.

3. Results and discussion

3.1. Calculation of the refractive index and film thickness

The optical system under consideration corresponds to homogeneous and uniform thin films, deposited on thick transparent substrates. The thermally evaporated films have thickness d and complex refractive index $n_c = n - ik$, where n is the refractive index and k is the extinction coefficient. The thickness of the substrate is several orders of magnitude larger than d, and its refractive index is symbolized by s ($s = (1/T_s) + \sqrt{(1/T_s^2) - 1}$, where T_s is the measured glass transmittance [12]). The substrate is considered to be perfectly smooth, but thick enough so that in practice the planes are not perfectly parallel so all interference effects arising from the substrate are destroyed. The system is surrounded by air with refractive index $n_o = 1$. Taking all the multiple reflections at the three interfaces into account, it can be shown that in the case $k^2 \ll n^2$, the transmission T at normal incidence is given by [13–15]:

$$T = \frac{Ax}{B - Cx\ \cos(\phi) + Dx^2} \tag{1}$$

where $A = 16n^2 s$, $B = (n+1)^3(n+s^2)$, $C = 2(n^2-1)\ (n^2-s^2)$, $D = (n-1)^3(n-s^2)$, $\phi = 4\pi nd/\lambda$ and $x = \exp(-\alpha d)$. The values of the transmission at the maxima and minima of the interference fringes can be obtained from Eq. (1) by setting the interference condition $\cos\phi = +1$ for maxima (T_M) and $\cos\phi = -1$ for minima (T_m).

Fig. 1 shows the measured transmittance (T) spectra, the created envelopes, T_M and T_m, and the geometric mean, $T_\alpha = \sqrt{T_M T_m}$, in the spectral region with interference fringes for the $Se_{82-x}Te_{18}Sb_x$ ($x = 0$, 3, 6 and 9 at.%) thin films, according to Swanepoel's method based on the idea of Manifacier et al. [16]. The first approximate value of the refractive index of the film, n_1, in the spectral region of medium and weak absorption can be calculated from the following expression:

$$n_1 = \sqrt{N + \sqrt{N^2 - s^2}} \tag{2}$$

where

$$N = 2s\frac{T_M - T_m}{T_M T_m} + \frac{s^2+1}{2}$$

Here T_M and T_m are the transmission maximum and the corresponding minimum at a certain wavelength λ. Alternatively, one of these values is an experimental interference maximum (minimum) and the other one is derived from the corresponding envelope. Both envelopes being computer-generated using the OriginLab (version 7) program.

The calculated values of the refractive index, n_1, using Eq. (2) are listed in Table 1. The accuracy of this initial estimation of the refractive index is improved after calculating d, as will be explained below. Now, it is necessary to take into account the basic equation

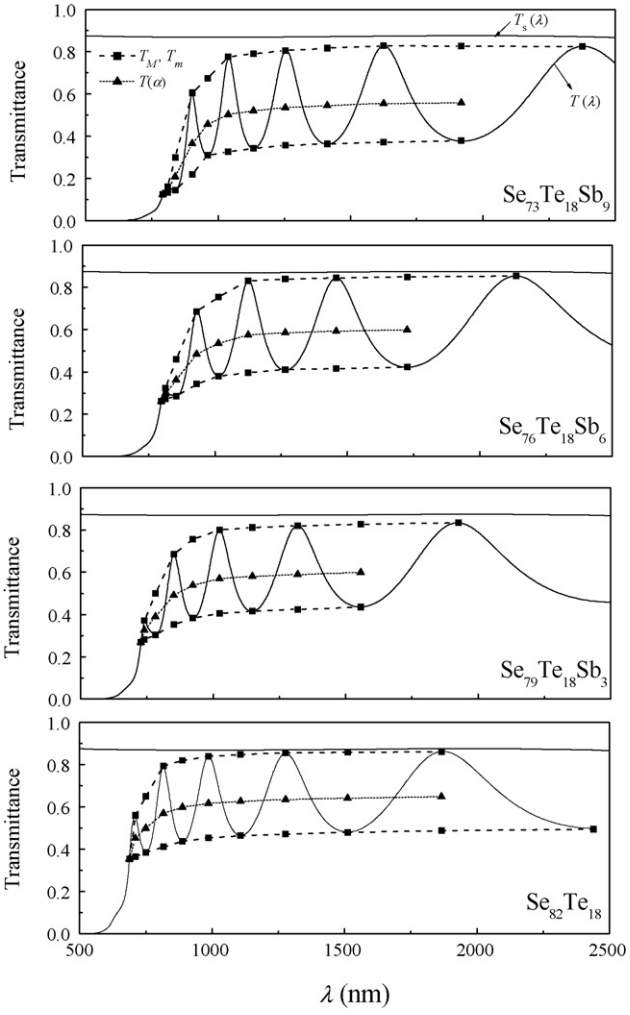

Fig. 1. Transmission spectra of $Se_{82-x}Te_{18}Sb_x$ ($x = 0$, 3, 6 and 9 at.%) thin films. The average thicknesses of these samples are 601, 585, 632 and 655 nm for $x = 0$, 3, 6 and 9 at.% respectively. Curves T_M, T_m and T_α according to the text. T_s is the transmission of the substrate alone.

for the interference fringes:

$$2nd = m_o\lambda \tag{3}$$

where the order number, m_o, is an integer for maxima and a half-integer for minima. Moreover, if n_{c1} and n_{c2} are the refractive indices at two adjacent maxima (or minima) at λ_1 and λ_2, then the film thickness can be expressed as:

$$d = \frac{\lambda_1\lambda_2}{2(n_{c2}\lambda_1 - n_{c1}\lambda_2)} \tag{4}$$

The values of d determined by this equation for different samples are listed as d_1 in Table 1. The last value deviates considerably from the other values and must consequently be rejected. The average value $\overline{d_1}$ of d_1 (ignoring the last value) can now be used, along with n_1, to calculate m_o for the different maxima and minima using Eq. (3). The accuracy of the film thickness can now be significantly increased by taking the corresponding exact integer or half-integer values of m_o associated with each extreme point (see Fig. 1) and deriving a new thickness, d_2. The values of the thickness in this way have a smaller dispersion. It should be emphasized that the accuracy of the final thickness is better than 1% (see Table 1).

With the accurate values of m_o and the average value $\overline{d_2}$ of d_2, Eq. (3) can then be solved for n at each λ and, thus, the

Table 1
Values of λ, T_s, T_M, T_m, n_1, d_1, m_o, d_2 and n_2 for $Se_{82-x}Te_{18}Sb_x$ (x = 0, 3, 6 and 9 at.%) thin films from transmission spectra of Fig. 1

Composition	λ	T_s	T_M	T_m	n_1	d_1	m_o	m	d_2	n_2
$Se_{82}Te_{18}$	1866	0.875	0.861	0.487	3.102		2.01	2.0	601	3.110
	1512	0.872	0.859	0.479	3.150		2.51	2.5	600	3.150
	1278	0.870	0.856	0.471	3.195	597	3.01	3.0	600	3.195
	1108	0.869	0.848	0.463	3.228	602	3.51	3.5	601	3.232
	986	0.869	0.840	0.453	3.269	613	3.99	4.0	603	3.287
	888	0.869	0.820	0.437	3.324	603	4.51	4.5	601	3.330
$\bar{d}_1 = 604$, $\delta_1 = 4.24$ nm (0.7%); $\bar{d}_2 = 601$, $\delta_1 = 1.1$ nm (0.18%)										
$Se_{79}Te_{18}Sb_3$	1558	0.873	0.827	0.435	3.328		2.51	2.5	585	3.329
	1320	0.871	0.820	0.424	3.390		3.01	3.0	584	3.385
	1148	0.869	0.812	0.415	3.436	583	3.51	3.5	585	3.434
	1024	0.869	0.801	0.404	3.488	597	3.99	4.0	587	3.501
	924	0.869	0.756	0.383	3.549	590	4.51	4.5	586	3.554
	852	0.869	0.686	0.352	3.640	577	5.02	5.0	585	3.641
$\bar{d}_1 = 587$, $\delta_1 = 4.24$ nm (.72%); $\bar{d}_2 = 585$, $\delta_1 = 1.03$ nm (0.17%)										
$Se_{76}Te_{18}Sb_6$	1726	0.874	0.850	0.423	3.422		2.52	2.5	631	3.429
	1458	0.872	0.845	0.416	3.467		3.02	3.0	631	3.466
	1266	0.870	0.839	0.410	3.502	638	3.52	3.5	633	3.511
	1126	0.869	0.832	0.396	3.582	622	4.05	4.0	629	3.569
	1014	0.867	0.754	0.380	3.566	666	4.47	4.5	640	3.616
	932	0.869	0.686	0.342	3.721	616	5.08	5.0	626	3.693
$\bar{d}_1 = 636$, $\delta_1 = 15.56$ nm (2.44%); $\bar{d}_2 = 632$, $\delta_1 = 4.72$ nm (0.74%)										
$Se_{73}Te_{18}Sb_9$	1918	0.875	0.826	0.378	3.658		2.46	2.5	655	3.660
	1626	0.874	0.828	0.371	3.717		2.95	3.0	656	3.724
	1412	0.871	0.817	0.364	3.760	662	3.44	3.5	657	3.773
	1254	0.870	0.805	0.356	3.808	666	3.92	4.0	657	3.829
	1134	0.869	0.790	0.342	3.895	648	4.43	4.5	655	3.895
	1038	0.869	0.775	0.325	4.010	605	4.98	5.0	647	3.962
$\bar{d}_1 = 645$, $\delta 1 = 40.3$ nm (6.2%); $\bar{d}_2 = 655$, $\delta_1 = 3.78$ nm (0.58%)										

The underlined values of transmittance are those given in the transmittance spectra of Fig. 1 and the others are calculated by the envelope method.

final values of the refractive index, n_2, are obtained. These values are listed in Table 1. Fig. 2 illustrates the dependence of the refractive index, n, on wavelength for different compositions of the amorphous $Se_{82-x}Te_{18}Sb_x$ (x = 0, 3, 6 and 9 at.%) thin films. Now, the values of n_2 can be fitted to a function such as the two-terms Cauchy dispersion relationship [17], $n(\lambda) = a + (b/\lambda^2)$, which can then be used to extrapolate the wavelength dependence beyond the range of measurement (see Fig. 2). This figure shows that the refractive index increases with increasing Sb content, over the entire spectral range studied. This increase is related to the increased polarizability of the larger Sb atoms (atomic radius, 136 pm), in comparison with Se atoms (atomic radius, 114 pm) [7].

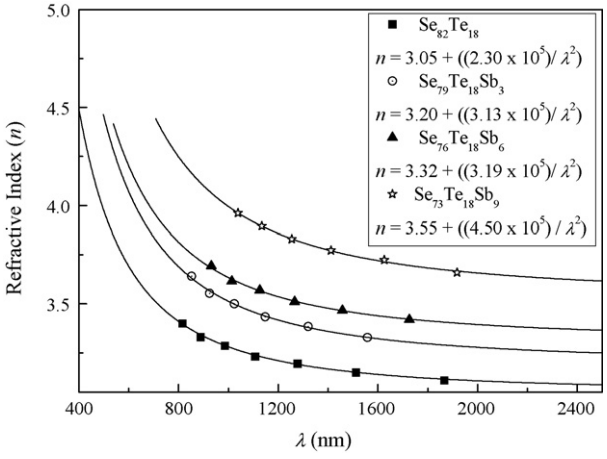

Fig. 2. Refractive index dispersion spectra for $Se_{82-x}Te_{18}Sb_x$ (x = 0, 3, 6 and 9 at.%) thin films. Solid curves are determined according to Cauchy dispersion relationship [17].

Furthermore, a simple complementary graphical method for deriving the first-order number, m_1, and film thickness, d, based on Eq. (3) was also used. For this purpose Eq. (3) can now be written for the extremes of the spectrum as:

$$\frac{l}{2} = 2d\left(\frac{n}{\lambda}\right) - m_1 \tag{5}$$

where l = 0, 1, 2, 3, ... for the successive tangent points, starting from the long wavelength end and m_1 is the order number of the first (l = 0) tangent point considered, where m_1 is an integer or a half-integer for the upper or lower tangent points, respectively. Therefore, by plotting (l/2) versus (n/λ) we obtain a straight line with slope 2d and cut-off on the vertical axis at $-m_1$. Fig. 3 shows this plot, in which the values obtained for d and m_1 are displayed for each sample.

According to Ioffe and Regel [18], the bonding character in the nearest-neighbour region, which means the coordination number; characterizes the electronic properties of the semiconducting materials. The coordination number obeying the so-called 8-N rule, where N is the valency of an atom. According to this rule the numbers of the nearest-neighbour atoms for Se, Te, and Sb are 2, 2 and 3, respectively. The average coordination number, N_r, for $Se_{82-x}Te_{18}Sb_x$ can be expressed as:

$$N_r = 2X\mathrm{Se} + 3X\mathrm{Sb} + 2X\mathrm{Te} \tag{6}$$

where X is the mole fraction. The coordination number increases with increasing the Sb content. The values of the coordination number and the excess of Se–Se homopolar bonds for the $Se_{82-x}Te_{18}Sb_x$ (x = 0, 3, 6 and 9 at.%) films are listed in Table 2.

The final values of the refractive index can be fitted to an appropriate function such as the Wemple–DiDomenico (WDD) dis-

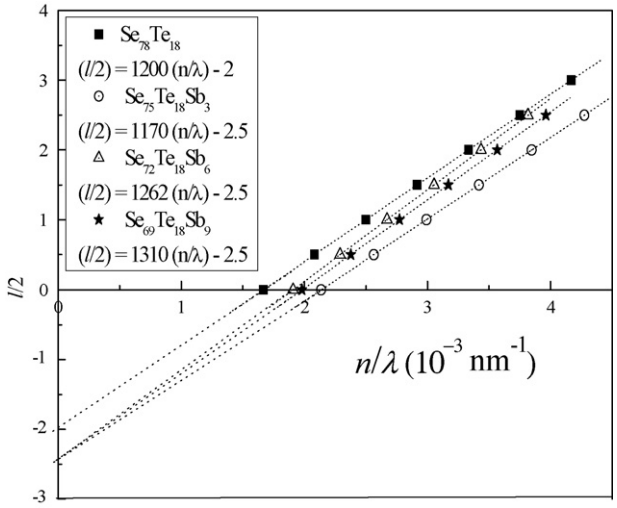

Fig. 3. Plots of (l/2) vs. (n/() to determine the film thickness and the first-order number, m_1, for $Se_{82-x}Te_{18}Sb_x$ (x = 0, 3, 6 and 9 at.%) thin films.

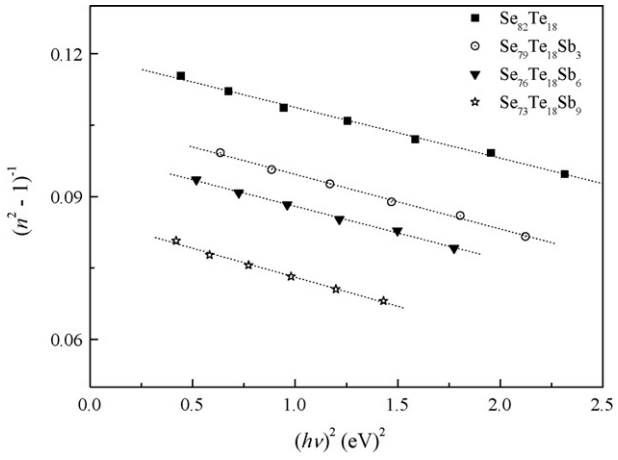

Fig. 4. Plots of refractive index factor $(n^2-1)^{-1}$ vs. $(h\nu)^2$ for $Se_{82-x}Te_{18}Sb_x$ (x = 0, 3, 6 and 9 at.%) thin films.

persion relationship [19], i.e., to the single-oscillator model:

$$n^2(h\nu) = 1 + \frac{E_o E_d}{E_o^2 - (h\nu)^2} \quad (7)$$

where E_o is the single-oscillator energy and E_d is the dispersion energy or single-oscillator strength. By plotting $(n^2-1)^{-1}$ against $(h\nu)^2$ and fitting straight lines (as shown in Fig. 4), E_o and E_d can be determined from the intercept E_o/E_d and the slope $(E_o E_d)^{-1}$. Fig. 4 also shows the values of the refractive index $n(0)$ at $h\nu = 0$ for the $Se_{82-x}Te_{18}Sb_x$ (x = 0, 3, 6 and 9 at.%) thin films. The obtained values of E_o, E_d and $n(0)$ are listed in Table 2. It was observed that, the single-oscillator energy decreases while the dispersion energy and the refractive index $n(0)$ increase with the increase of Sb content. The oscillator energy, E_o, is the average energy gap parameter and with a good approximation it varies in proportion to optical band gap ($E_o \approx 2E_g$) [20]. The dispersion energy or single-oscillator strength, E_d, serves as a measure of the strength of interband transitions [21]. E_d increases with increasing Sb content as antimony is more coordinated in the matrix.

An important achievement of the WDD model is that it relates the dispersion energy, E_d, to other physical parameters of the material through the following empirical relationship [19]:

$$E_d = \beta N_c Z_a N_e \ \text{(eV)} \quad (8)$$

where N_c is the effective coordination number of the cation nearest-neighbour to the anion, Z_a is the formal chemical valency of the anion, N_e is the effective number of valence electrons per anion and $\beta = 0.37 \pm 0.04$ eV for covalent crystalline and amorphous materials. The increase of E_d value means increase of the average cation coordination number with increasing Sb content.

The dependence of the refractive index, n, on the lattice dielectric constant, ε_L, is given by [22]:

$$n^2 = \varepsilon_L - \left(\frac{e^2}{\pi c^2}\right)\left(\frac{N}{m^*}\right)\lambda^2 \quad (9)$$

where N/m^* is the ratio of the carrier concentration, N, to the effective mass, m^*, c is the speed of light, and e is the electronic charge. The plots of n^2 versus λ^2 as shown in Fig. 5 are linear, verifying Eq. (9). The values of ε_L and N/m^* were deduced from the extrapolation of these plots to $\lambda^2 = 0$ and from the slope of the graph respectively. The obtained values of ε_L and N/m^* for the $Se_{82-x}Te_{18}Sb_x$ (x = 0, 3, 6 and 9 at.%) thin films are listed in Table 2.

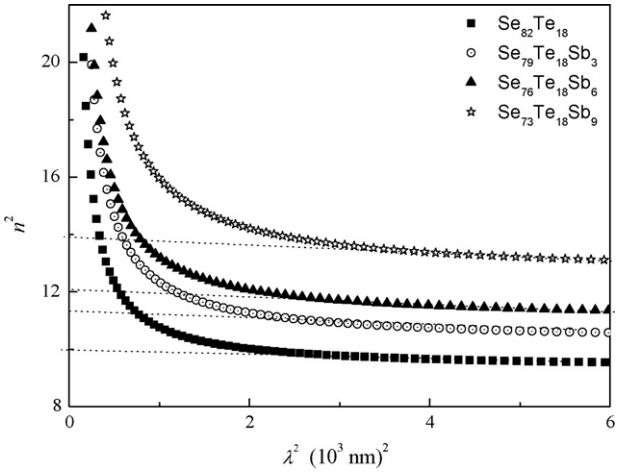

Fig. 5. Plots of n^2 vs. λ^2 for $Se_{82-x}Te_{18}Sb_x$ (x = 0, 3, 6 and 9 at.%) thin films.

Table 2
Wemple–DiDomenico dispersion parameters (E_o and E_d), E_o/E_g ratio, values of the refractive index extrapolated at $h\nu = 0$, the excess of Se–Se homopolar bonds, the coordination number, the cohesive energy, the lattice dielectric constant and the N/m^* ratio for $Se_{82-x}Te_{18}Sb_x$ (x = 0, 3, 6 and 9 at.%) thin films

Composition	E_o (eV)	E_d (eV)	E_o/E_g	$n(0)$	Excess Se–Se	N_r	CE eVatom^{-1}	N/m^* (10^{44}/cm^3)	ε_L
$Se_{82}Te_{18}$	3.33	28.02	2.06	3.07	64	2.00	1.90	0.77	9.9
$Se_{79}Te_{18}Sb_3$	3.04	28.67	2.07	3.23	56	2.03	1.93	1.19	11.2
$Se_{76}Te_{18}Sb_6$	2.97	30.02	2.14	3.33	49	2.06	1.96	1.32	11.9
$Se_{73}Te_{18}Sb_9$	2.64	31.01	2.10	3.57	41	2.09	1.99	1.59	13.9

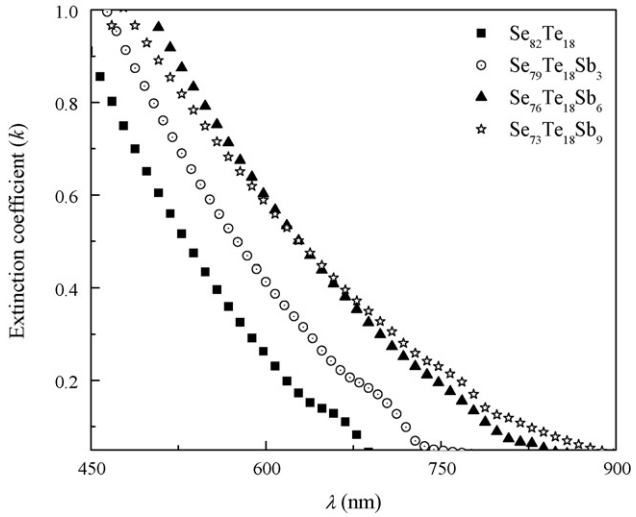

Fig. 6. Extinction coefficient, k, vs. λ for $Se_{82-x}Te_{18}Sb_x$ (x = 0, 3, 6 and 9 at.%) thin films.

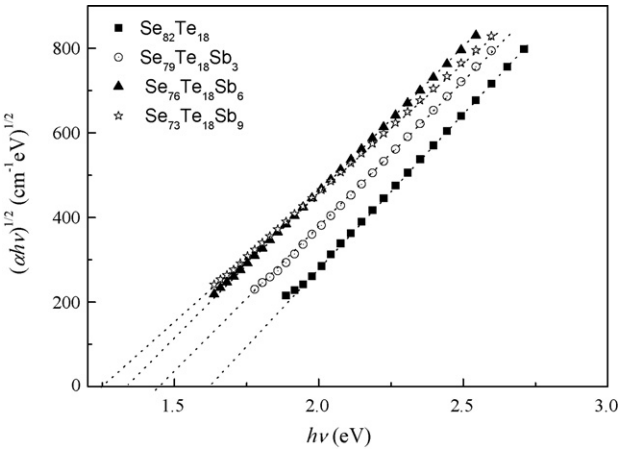

Fig. 7. Dependence of $(\alpha h\nu)^{1/2}$ on photon energy ($h\nu$) for $Se_{82-x}Te_{18}Sb_x$ (x = 0, 3, 6 and 9 at.%) thin films from which the optical band gap, E_g, is estimated (Tauc extrapolation).

3.2. Determination of the extinction coefficient and optical band gap

Continuing with the description of the data processing method, when there is no substrate in the reference beam and the values of the refractive index, n, and the thickness, d, of the films are already known, the absorption coefficient α is derived using the interference-free transmission spectrum T_α (see Fig. 1) over the whole spectral range, using the well-known equation suggested by Connell and Lewis [23]:

$$\alpha = -\frac{1}{d}\ln\left(\frac{1}{B}\{A + [A^2 + 2BT_\alpha(1-R_2R_3)]^{1/2}\}\right) \quad (10)$$

where $A = (R_1 - 1)(R_2 - 1)(R_3 - 1)$, $B = 2T_\alpha(R_1R_2 + R_1R_3 - 2R_1R_2R_3)$, R_1 is the reflectance of the air–film interface ($R_1 = [(1-n)/(1+n)]^2$), R_2 is the reflectance of film–substrate interface ($R_2 = [(n-s)/(n+s)]^2$) and R_3 is the reflectance of the substrate–air interface ($R_3 = [(s-1)/(s+1)]^2$).

To complete the calculations of the optical constants, the extinction coefficient, k, is calculated using the values of α and λ by the already mentioned formula $k = \alpha\lambda/4\pi$. Fig. 6 shows the extinction coefficient as a function of the wavelength for $Se_{82-x}Te_{18}Sb_x$ (x = 0, 3, 6 and 9 at.%) thin films. It should be pointed out that the absorption coefficient of amorphous semiconductors, in the high-absorption region ($\alpha \geq 10^4\ cm^{-1}$), is given according to Tauc by the following equation [24]:

$$\alpha(h\nu) = \frac{B(h\nu - E_g)^2}{h\nu} \quad (11)$$

where $h\nu$, B and E_g are the photon energy, a parameter that depends on the transition probability and the optical bang gap, respectively. Fig. 7 shows the absorption coefficient in the form of $(\alpha h\nu)^{1/2}$ versus ($h\nu$) for $Se_{82-x}Te_{18}Sb_x$ (x = 0, 3, 6 and 9 at.%) thin films. The intercepts of the straight lines with the photon energy axis yield the values of the optical band gap. Continuing with the analysis of the optical absorption edge, at lower values of the absorption coefficient ($\alpha \leq 10^4\ cm^{-1}$), the absorption depends exponentially on the photon energy (the so-called Urbach relation [25])

$$\alpha(h\nu) = \alpha_0 \exp\left(\frac{h\nu}{E_e}\right) \quad (12)$$

where α_0 is a constant and E_e is the Urbach energy (related to the width of the band tail of the localized states at the conduction or valence band edge). The effect of Sb content on the optical gap, E_g, and the Urbach energy, E_e, for $Se_{82-x}Te_{18}Sb_x$ (x = 0, 3, 6 and 9 at.%) thin films is shown in Fig. 8, from which one can observe that, the decrease in E_g with increasing Sb content can be described by an empirical formula:

$$E_g = 1.052 + 0.571\left(\exp\left(\frac{-x}{8.74}\right)\right) \quad (13)$$

also the increase in E_e with increasing Sb content can be written in the form:

$$E_e = 0.077 - 0.067\left(\exp\left(\frac{-x}{21.75}\right)\right) \quad (14)$$

where x is the Sb content (at.%). The decrease in E_g of amorphous films can be explained by the increased tailing of the band tails in the gap [26] (see Fig. 8).

According to the chemical-bond approach [27,28], bonds are formed in the sequence of decreasing bond energy until the available valence of atoms is satisfied. The bond energies $D(A-B)$ for heteronuclear bonds have been calculated by using the empirical relation

$$D(A-B) = [D(A-A)D(B-B)]^{1/2} + 30(\chi_A - \chi_B)^2 \quad (15)$$

proposed by Pauling [29], where $D(A-A)$ and $D(B-B)$ are the energies of the homonuclear bonds (44.04, 30.22 and 33 kcal mol^{-1} for

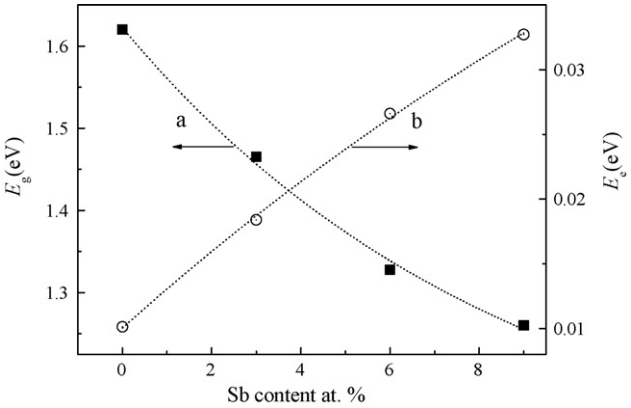

Fig. 8. Variation in the optical band gap, E_g, and the width of localized states, E_e, as a function of Sb content for $Se_{82-x}Te_{18}Sb_x$ (x = 0, 3, 6 and 9 at.%) thin films.

Se, Sb and Te, respectively) [29], χ_A and χ_B are the electronegativity values for the involved atoms (2.55, 2.05 and 2.1 for Se, Sb and Te, respectively) [29]. In the present compositions, the Se–Te bonds with the highest possible energy (44.2 kcal mol^{-1}) are expected to form first, then Sb–Se (43.97 kcal mol^{-1}) to saturate all available valence of Se. There are still unsatisfied Se valences which must be satisfied by the formation of Se–Se bonds. Based on the chemical-bond approach, the bond energies are assumed to be additive. Thus, the cohesive energies were estimated by summing the bond energies over all the bonds expected in the material. The calculated values of the cohesive energies for all compositions are presented in Table 2. These results indicate that, the cohesive energies of these glasses increase with increasing Sb content.

In connection with the values of the tail width (E_e), it is seen that, the increase of Sb content leads to an increase in E_e. The increase of CE implies a higher bonding strength, i.e. low E_g (higher in defect bonds) which increase the band tail width. Hurst and Davis [30] explained these results by suggesting that when the bond energies in the alloy are not very different (Se–Te and Sb–Se bond in our case), the increase in disorder associated with the deviation from stoichiometry will tend to push the mobility edges further into the bands, thereby decreasing E_g.

4. Conclusions

Optical characterization of $Se_{82-x}Te_{18}Sb_x$ thin films have been analyzed based on the generation of the envelopes of the interference maxima and minima of the transmission spectrum (Swanepoel's method). The allowed non-direct electronic transitions are mainly responsible for the photon absorption in the investigated films. Fitting the refractive indices, according to single-oscillator model, result in dispersion parameters that are directly related to the structure of the films. It was found that the optical band gap, E_g, and the single-oscillator energy, E_o, decrease while the refractive index, n, and the dispersion energy, E_d, increase by increasing Sb content. The chemical-bond approach has been applied successfully to interpret the observed decrease of the optical gap of $Se_{82-x}Te_{18}Sb_x$ films with increasing Sb content.

Acknowledgment

The authors thank Al-Azhr University for the financial support.

References

[1] M. Horie, T. Ohno, N. Nobukuni, K. Kioyo, T. Hahizume, Tech. Digest, ODS2001 MC1, 2001, p. 37.
[2] T. Akiyama, M. Uno, H. Kituara, K. Narumi, K. Nishiuchi, N. Yamada, Jpn. J. Appl. Phys. 40 (2001) 1598.
[3] T. Ohta, J. Opto-electron. Adv. Mater. 3 (2001) 609.
[4] S.O. Kasap, T. Wagner, V. Aiyah, O. Krylouk, A. Bekirov, L. Tichy, J. Mater. Sci. 34 (1999) 3779.
[5] A. Dahshan, J. Non-Cryst. Solids 354 (2008) 3034.
[6] A. Dahshan, H.H. Amer, A.H. Moharram, A.A. Othman, Thin Solid Films 513 (2006) 369.
[7] A.H. Moharram, A.A. Othman, H.H. Amer, A. Dahshan, J. Non-Cryst. Solids 352 (2006) 2187.
[8] E. Marquez, T. Wagner, J.M. Gonzalez-Leal, A.M. Bernal-Olive, R. Prieto-Aleon, R. Jimenez-Garay, P.J.S. Ewen, J. Non-Cryst. Solids 274 (2000) 62.
[9] R. Swanepoel, J. Phys. E: Sci. Instrum. 16 (1983) 1214.
[10] R. Swanepoel, J. Phys. E: Sci. Instrum. 17 (1984) 896.
[11] T.I. Kosa, T. Wagner, P.J.S. Ewen, A.E. Owen, Philos. Mag. B 71 (1995) 311.
[12] F.A. Jenkins, H.E. White, Fundamentals of Optics, McGraw-Hill, New York, 1957.
[13] E. Marquez, A.M. Bernal-Oliva, J.M. Gonzalez-Leal, R. Prieto-Alcon, R. Jimenez-Garay, J. Non-Cryst. Solids 222 (1997) 250.
[14] K.A. Aly, A. Dahshan, A.M. Abousehly, Philos. Mag. 88 (1) (2008) 47.
[15] S. Heavens, Optical Properties of Thin Solid Films, Butterworths, London, 1955.
[16] J.C. Manifacier, J. Gasiot, J.P. Fillard, J. Phys. E: Sci. Instrum. 9 (1976) 1002.
[17] T.S. Moss, Optical Properties of Semiconductors, Butterworths, London, 1959.
[18] A.F. Ioffe, A.R. Regel, Prog. Semicond. 4 (1960) 239.
[19] S.H. Wemple, M. DiDomenico, Phys. Rev. B 3 (1971) 1338.
[20] K. Tanaka, Thin Solid Films 66 (1980) 271.
[21] M. Krbal, T. Wagner, Mil. Vlcek, Mir. Vlcek, M. Frumar, J. Non-Cryst. Solids 352 (2006) 2662.
[22] G. Kumar, J. Thomas, N. George, B. Kumar, P. Shnan, V. Npoori, C. Vallabhan, N. Unnikrishnan, Phys. Chem. Glasses 41 (2001) 89.
[23] G.A.N. Connell, A.J. Lewis, Phys. Status Solidi (B) 60 (1973) 291.
[24] J. Tauc, in: J. Tauc (Ed.), Amorphous and Liquid Semiconductors, Plenum, New York, 1974.
[25] F. Urbach, Phys. Rev. B 92 (1953) 1324.
[26] P. Nagel, L. Tichy, A. Triska, H. Ticha, J. Non-Cryst. Solids 59/60 (1983) 1015.
[27] J. Bicermo, S.R. Ovshinsky, J. Non-Cryst. Solids 74 (1985) 75.
[28] B. Jozef, O. Stanford, S. Mahadevan, A. Gridhar, A.K. Singh, J. Non-Cryst. Solids 74 (1985) 75.
[29] J. Pauling, Nature of the Chemical Bond, Cornell University Press, Ithaca, NY, 1960.
[30] Ch. Hurst, E.A. Davis, in: J. Stuke, W. Brenig (Eds.), Amorphous and Liquid Semiconductors, Taylor and Francis, London, 1974.